

Seeing Through the Chain: Mitigate Hallucination in Multimodal Reasoning Models via CoT Compression and Contrastive Preference Optimization

Hao Fang ^{* 1} Jinyu Li ^{* 2} Jiawei Kong ¹ Tianqu Zhuang ¹ Kuofeng Gao ¹
 Bin Chen ² Shu-Tao Xia ¹ Yaowei Wang ²

Abstract

While multimodal reasoning models (MLRMs) have exhibited impressive capabilities, they remain prone to hallucinations, and effective solutions are still underexplored. In this paper, we experimentally analyze the hallucination cause and propose C3PO, a training-based mitigation framework comprising Chain-of-Thought Compression and Contrastive Preference Optimization. Firstly, we identify that introducing reasoning mechanisms exacerbates models' reliance on language priors while overlooking visual inputs, which can produce CoTs with reduced visual cues but redundant text tokens. To this end, we propose to selectively filter redundant thinking tokens for a more compact and signal-efficient CoT representation that preserves task-relevant information while suppressing noise. In addition, we observe that the quality of the reasoning trace largely determines whether hallucination emerges in subsequent responses. To leverage this insight, we introduce a reasoning-enhanced preference tuning scheme that constructs training pairs using high-quality AI feedback. We further design a multimodal hallucination-inducing mechanism that elicits models' inherent hallucination patterns via carefully crafted inducers, yielding informative negative signals for contrastive correction. We provide theoretical justification for the effectiveness and demonstrate consistent hallucination reduction across diverse MLRMs and benchmarks.

1. Introduction

Large Reasoning Models such as DeepSeek-R1 (Guo et al., 2025) have recently demonstrated remarkable problem-solving capabilities across a wide range of practical and

^{*}Equal contribution ¹Tsinghua University ²Harbin Institute of Technology, Shenzhen. Correspondence to: Bin Chen <chen-bin21@hit.edu.cn>.

Preprint. February 4, 2026.

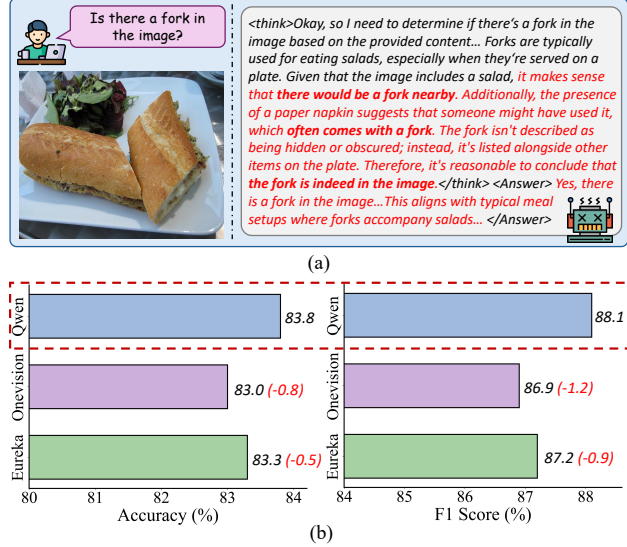


Figure 1. (a) A hallucination case from R1-Onevision (Yang et al., 2025a). (b) Performance of MLRMs R1-Onevision and MM-Eureka (Meng et al., 2025) and the base model Qwen2.5-VL-7B (Bai et al., 2025b) on the hallucination benchmark AMBER (Wang et al., 2023), where *high values indicate fewer hallucinations*. The hallucination increases from the base model to reasoning variants.

complex scenarios. Motivated by these advances, a growing number of studies have sought to extend such powerful multi-step reasoning mechanisms to multimodal settings by applying supervised fine-tuning (SFT) or reinforcement learning (RL) to multimodal models. Benefiting from meticulous chain-of-thought (CoT) supervision, Multimodal Large Reasoning Models (MLRMs) have achieved impressive performance on challenging tasks, such as visual mathematics problem-solving (Wang et al., 2025).

Despite recent progress, hallucination remains a persistent issue for MLRMs, which may generate semantically plausible yet factually incorrect or visually irrelevant content, as illustrated in Figure 1(a). More strikingly, evaluation of representative MLRMs and the corresponding base models on a commonly used hallucination benchmark reveals that MLRMs can hallucinate even more severely than their non-reasoning counterparts. This is a counterintuitive phenomenon, as the presence of logical, structured reasoning should, in principle, facilitate a more detailed perception

of the image and hence yield more faithful and image-grounded answers. These observations underscore the need for a deeper understanding of hallucinations specific to MLRMs and the development of mitigation strategies.

However, existing studies primarily focus on constructing benchmarks to better evaluate MLRM’s hallucinations and influential factors (Liu et al., 2025), or exclusively discuss the self-contradictory reasoning within CoT traces (Dong et al., 2025a), leaving approaches for hallucination mitigation in general multimodal tasks largely underexplored.

In this work, we conduct two hallucination-analysis experiments tailored to the unique characteristics of MLRMs and identify two key factors contributing to their hallucinations. Based on these insights, we propose C3PO, a two-stage hallucination mitigation framework specifically designed for MLRMs via CoT Compression and Contrastive Preference Optimization. We begin by analyzing the attention distribution of MLRMs and observe that introducing explicit reasoning mechanisms causes models to allocate even less attention to visual tokens than their non-reasoning counterparts. As a result, MLRMs tend to over-rely on language priors rather than grounding in visual inputs. This issue weakens visual signals in the generated CoTs and introduce unnecessary text tokens. From the Information Bottleneck (IB) view (Tishby et al., 2000; Tishby & Zaslavsky, 2015), the reasoning chain serves as an intermediate representation between visual inputs and final answers, which should preserve critical visual cues relevant to the answer while discarding redundant or noisy content. Motivated by this, we propose a simple yet effective method that selectively filters low-importance reasoning tokens to produce a more compact and signal-efficient representation, which is theoretically justified under the IB framework. Remarkably, this strategy reduces hallucinations without introducing any additional supervision, validating the rationality of our design.

Next, we investigate the causal relationship of hallucinations from reasoning chains to final answers. Our analysis reveals a key finding that high-quality CoTs consistently lead to hallucination-free responses, whereas hallucinated CoTs substantially amplify the likelihood of hallucinations in the final answers. Building on this, we propose a reasoning-enhanced preference learning strategy based on direct preference optimization (DPO). Specifically, we leverage expert feedback from advanced MLLMs to enhance the quality of MLRM-generated CoTs. Data samples with the enhanced traces are used as positive samples, while the original outputs serve as negative ones. To further expose the model’s intrinsic hallucination behaviors, we introduce a multimodal hallucination-inducing mechanism that carefully crafts visual and textual inputs to elicit diverse hallucination patterns as additional negative contrasts. By performing contrastive preference tuning on AI-enhanced positives and intention-

ally induced hallucination negatives, the model is trained to generate more reliable and coherent reasoning chains, substantially reducing hallucinations in final responses.

Contributions. We first uncover the hallucination mechanisms specific to the unique reasoning process of MLRMs. Based on these analyses, we propose C3PO, a two-stage hallucination mitigation framework for MLRMs that first leverages SFT to compress redundant CoT tokens, and then performs a reasoning-enhanced contrastive preference optimization (CPO) using high-quality preference pairs derived from AI feedback. In addition, we introduce a multimodal hallucination-inducing technique that exploits the inherent failure behaviors of MLRMs as informative contrastive references. Furthermore, we develop a theoretical framework from an information-bottleneck perspective that provides principled justification for the superiority of C3PO.

To validate the effectiveness, we conduct comprehensive experiments on various MLRMs across a wide range of benchmarks, which demonstrate that the proposed framework substantially reduces MLRMs’ hallucinations.

Related work. We discuss related studies in Appendix D.

2. Understanding Hallucination in MLRMs

In this section, we conduct preliminary analyses tailored to the unique characteristics of MLRMs to uncover potential causes of hallucinations, which subsequently guide the principled design of our mitigation framework.

A key distinction between MLRMs and conventional multimodal large language models (MLLMs) lies in the explicit incorporation of CoT reasoning. Centered on this distinctive mechanism, we investigate two fundamental questions that are closely tied to hallucination behaviors in MLRMs:

- **Q1:** *How does the introduction of a reasoning process affect attention allocation? Does reasoning encourage more attention to visual inputs, or instead reduce them?*
- **Q2:** *Does hallucination in the reasoning chain causally propagate to the final answer, and can hallucination-free reasoning reliably ensure hallucination-free answers?*

Question 1. Previous studies (Favero et al., 2024; Fang et al., 2025) have shown that a primary cause of hallucinations is models’ tendency to allocate excessive attention to text tokens while insufficient attention to critical visual inputs. As a result, the responses are more influenced by the language priors rather than the actual image input.

The attention analysis in Fig. 2(a) shows that reasoning models further exacerbate attention bias. Compared to their non-reasoning base models, MLRMs significantly decrease attention to visual tokens while allocating even more attention to textual tokens. This shift amplifies the imbalance

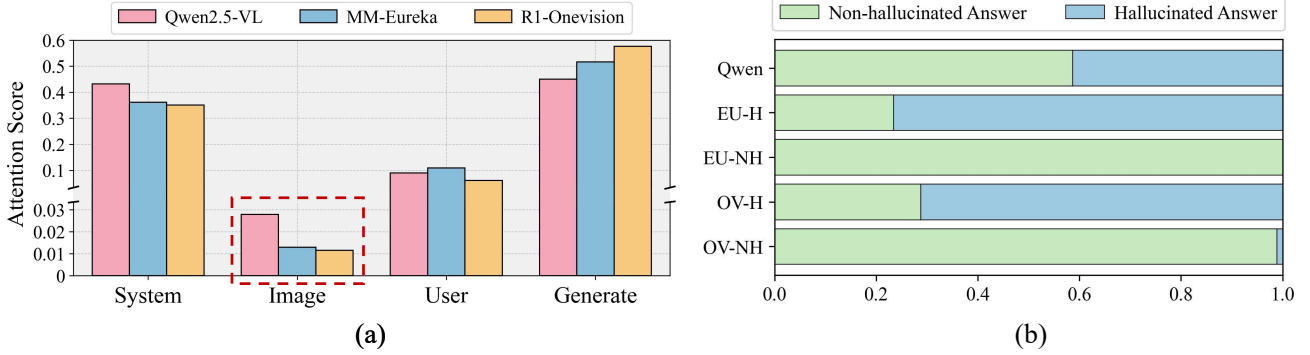


Figure 2. Illustration of two important hallucination analyses for MLRMs. (a) Attention distributions of representative MLRMs and the non-reasoning base model Qwen2.5-VL averaged on 300 samples from MSCOCO (Lin et al., 2014). Compared to Qwen2.5-VL, MLRMs exhibit a substantial reduction in attention to visual tokens and a prominent increase in attention to textual tokens. (b) Proportion of hallucinated answers given hallucinated (-H) and non-hallucinated (-NH) CoTs under CHAIR (Rohrbach et al., 2018) evaluation. EU denotes MM-Eureka and OV denotes R1-Onevision. The hallucination rate of the base model Qwen2.5-VL is reported as a reference.

between visual grounding and language priors during generation, increasing the risk of hallucinations.

Summary 1. Introducing reasoning phrases decreases focus on visual tokens and amplifies reliance on textual priors, which can produce CoTs with diluted visual information and redundant text tokens. Building on the IB principle and empirical findings that many CoT tokens are redundant and irrespective of model decisions (Xia et al., 2025; Feng et al., 2025), we adopt a selective CoT token pruning strategy to enhance information flow and encourage reliable answers.

Question 2. The CoT chain plays a critical role in shaping the final answer in reasoning models. To investigate the potential causal relationship between hallucinations in the reasoning chain and those in the final answer, we explicitly decouple these two sources of hallucination under the CHAIR evaluation and conduct a causal analysis, as shown in Fig. 2(b). As expected, when the CoT is hallucinated, the majority of generated answers also exhibit hallucinated content, with a hallucination rate higher than that of the non-reasoning base model. This confirms that hallucinations in the CoT chain can strongly propagate to the final responses.

Another encouraging observation is that reliable reasoning chains almost always lead to hallucination-free answers, as high-quality reasoning enables more faithful analysis of the image and hence facilitates reliable answers. This provides preliminary evidence for the feasibility of mitigating hallucinations by enhancing the quality of reasoning chains.

Summary 2. Hallucinated CoTs increase the likelihood of hallucinations in final answers, whereas reliable reasoning chains strongly suppress such errors. Accordingly, we employ preference optimization with a reasoning-centric objective, where we introduce AI-enhanced reasoning as positive supervision and deliberately induced hallucinated content as contrastive negatives.

3. Method

In this section, we present the proposed two-stage hallucination mitigation framework for MLRMs. We also provide a theoretical analysis from an IB perspective.

3.1. CoT Compression for Enhanced Visual Grounding

Based on our preliminary analysis, we aim to trim superfluous reasoning tokens with less importance in the reasoning chain. This is also consistent with the over-thinking issue in LRM (Chen et al., 2024; Li et al., 2025), where excessively long CoTs increase computational burdens and degrade model performance. Inspired by recent findings that LLMs can perform reliably with pruned CoTs (Xia et al., 2025), we implement compression by training the model to reason and predict based on trimmed reasoning traces.

Data Construction. Given a multimodal reasoning model f_θ , we query f_θ with image-question pairs (v, x) to generate reasoning chain z and final answer y . We then identify and remove reasoning tokens with limited impact on model predictions using importance scores provided by the powerful LLMlingua-2 (Pan et al., 2024), a token-level importance scoring model that has been widely adopted in prior compression studies (Pan et al., 2024; Xia et al., 2025).

Specifically, LLMlingua-2 is trained with GPT-4 annotations and is capable of assigning higher importance scores to semantically informative tokens (e.g., object attributes and scene descriptions in image captioning), while assigning lower scores to function words and transitional tokens with limited semantics and minimal influence on model decisions (See examples in Appendix E.1). Tokens are then ranked by importance, and the top γ percentile is retained to form the pruned chain z' . The resulting dataset of N samples is denoted as $\mathcal{D}_s = \{(x_{(i)}, v_{(i)}, z'_{(i)}, y_{(i)})\}_{i=1}^N$.

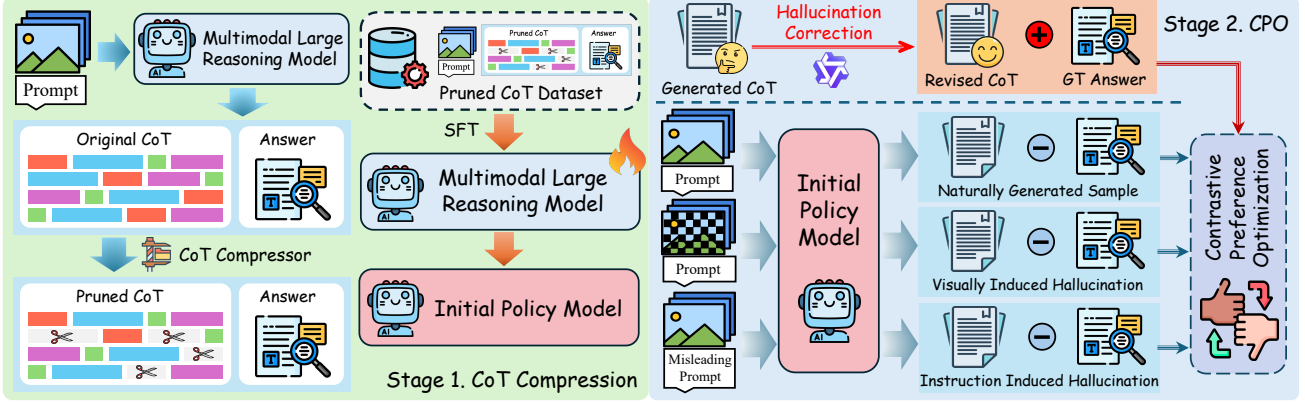


Figure 3. Overview of the proposed C3PO framework. We first construct SFT datasets by removing redundant tokens within the generated CoTs based on token importance scores. We then perform hallucination-aware preference optimization, where preferred samples contain enhanced reasoning traces via feedback from an advanced open-source MLLM, while the original unmodified outputs serve as rejected ones. Moreover, we propose a novel multimodal hallucination-inducing mechanism that crafts degraded visual inputs and misleading prompts to elicit MLRM’s inherent hallucination patterns as informative negative contrasts.

Model Training. We then use the constructed dataset \mathcal{D}_s to perform LoRA-based SFT on MLRMs, which trains the model to reason with compressed CoTs and generate faithful answers. The training objective can be expressed as:

$$\mathcal{L}_{\text{SFT}} = -\mathbb{E}_{(v, x, z', y) \sim \mathcal{D}_s} \sum_{t=1}^{l_{z'}} \log p_\theta(z'_t | v, x, z'_{<t}) + \sum_{t=1}^{l_y} \log p_\theta(y_t | v, x, z', y_{<t}), \quad (1)$$

where $l_{z'}$ and l_y denote the sequence lengths of z' and y , respectively. Notably, this SFT process does not introduce any additional supervision information beyond the model’s own outputs. We simply prune the generated reasoning chains and pair them with the original, unmodified answers for training. As shown in Table 6, this strategy already brings a notable reduction in hallucinations, confirming the rationality of our analysis and design.

3.2. Contrastive Preference Optimization

Motivated by the preceding analysis, we propose a preference optimization framework that effectively strengthens the reasoning process via high-quality preference data pairs.

To obtain robust CoT chains, we adopt the well-established RLAIF paradigm that constructs data by incorporating high-quality feedback from advanced MLLMs. The refinement task is decomposed into sentence-level hallucination detection and the correction problem (Yang et al., 2025b). This simplification allows open-source MLLMs to effectively handle the task and provide more reliable guidance.

Specifically, we condition the advanced Qwen3-VL (Bai et al., 2025a) on the input image v , the question x , and the ground-truth answer y_{GT} , and instruct it to revise the reasoning chain z_{Gen} generated by the MLRM f_θ . The model is instructed to identify and correct hallucinated content in the CoT at the sentence level, to improve the faithfulness of the reasoning trace to the visual input. Accordingly, the refined reasoning chain z_{Rev} is then used as the preferred sample and the original unmodified reasoning chains z_{Gen} that may contain hallucinations serve as inferior ones.

Multimodal Hallucination-Inducing Contrast. Beyond directly crafting high-quality positive samples, we further conduct a reverse-thinking analysis. While it is challenging to consistently derive hallucination-free responses from a given MLRM, eliciting the opposite hallucinated predictions is considerably easier. Such hallucinated samples are also highly valuable and informative as they explicitly expose the model’s intrinsic hallucination patterns, which can serve as negative references for contrastive preference optimization.

Therefore, we propose a multimodal hallucination-inducing mechanism that carefully crafts both visual and textual inputs to elicit outputs with rich hallucinated content. As shown in Fig. 3, we induce visual hallucinations by applying random masks to input images, which diminishes substantial ground-truth visual evidence and implicitly forces the model to rely on language priors, resulting in semantically coherent yet hallucinated CoT chains and answers ($z_{\text{img}}, y_{\text{img}}$). For the textual modality, we design a hallucination-amplification prompt (see Appendix B.1) that directly instructs the model to prioritize its language priors while partially ignoring the visual input to create a plausible-sounding hallucinated reasoning trace and answer ($z_{\text{ins}}, y_{\text{ins}}$). These two mechanisms effectively simulate MLRM’s hallucination behaviors commonly observed in real-world inference, providing informative negative samples that encourage the model to perceive and correct its intrinsic hallucination behaviors.

Reasoning-Enhanced Optimization. Given the preference dataset \mathcal{D}_p constructed by above operations, we enhance the thinking process by introducing a reasoning-centric preference loss, which encourages the model to favor reliable reasoning trajectories over inferior ones:

$$\begin{aligned} \mathcal{L}_{\text{RE}} = & -\mathbb{E}_{(v, x, z_{\text{Rev}}, \mathcal{N}_z) \sim \mathcal{D}_p} \\ & \sum_{z_l \in \mathcal{N}_z} \log \sigma \left[\beta r_\theta(z_{\text{Rev}} | v, x) - \beta r_\theta(z_l | v, x) \right], \end{aligned} \quad (2)$$

where $\mathcal{N}_z = \{z_{\text{Gen}}, z_{\text{img}}, z_{\text{ins}}\}$,

$$r_\theta(z | v, x) \triangleq \log \frac{p_\theta(z | v, x)}{p_{\theta_{\text{ref}}}(z | v, x)}.$$

Here the θ_{ref} denotes the parameters of the reference model. This design provides direct preference supervision on the reasoning process, which effectively stabilizes and facilitates the generation of faithful CoT chains, hence significantly reducing hallucinations in the subsequent answers.

However, optimizing reasoning preferences alone does not guarantee that the outputs consistently follow the desired (*reasoning, answer*) format, and may even degrade the coherence and quality of the final answer. To stabilize holistic generation behavior and explicitly improve answer quality, we further adopt a standard DPO objective that models preferences over the joint output (z, y) :

$$\begin{aligned} \mathcal{L}_{\text{DPO}} = & -\mathbb{E}_{(v, x, z_{\text{Rev}}, y_{\text{GT}}, \mathcal{N}) \sim \mathcal{D}_p} \\ & \sum_{(z_l, y_l) \in \mathcal{N}} \log \sigma \left[\beta r_\theta(z_{\text{Rev}}, y_{\text{GT}} | v, x) - \beta r_\theta(z_l, y_l | v, x) \right], \end{aligned}$$

where $\mathcal{N} = \{(z_{\text{Gen}}, y_{\text{Gen}}), (z_{\text{img}}, y_{\text{img}}), (z_{\text{ins}}, y_{\text{ins}})\}$,

$$r_\theta(z, y | v, x) \triangleq \log \frac{p_\theta(z, y | v, x)}{p_{\theta_{\text{ref}}}(z, y | v, x)}.$$

By conducting contrastive preferences over the holistic output distribution, we guide the model to generate well-formed and faithful responses with robust CoTs and final answers.

In addition, existing studies (Wang et al., 2024) have observed that the probability of preferred responses may decrease because DPO focuses on relative preferences. Similarly, we introduce the anchor regularization to constrain the positive reward above a predefined threshold δ :

$$\begin{aligned} \mathcal{L}_{\text{Anc}} = & -\mathbb{E}_{(v, x, z_{\text{Rev}}, y_{\text{GT}}) \sim \mathcal{D}_p} \left[\log \sigma \left(\beta r_\theta(z_{\text{Rev}} | v, x) - \delta \right) \right. \\ & \left. + \lambda_{\text{DPO}} \log \sigma \left(\beta r_\theta(z_{\text{Rev}}, y_{\text{GT}} | v, x) - \delta \right) \right], \end{aligned} \quad (4)$$

where λ_{DPO} is the hyperparameter that balances the contributions of two loss terms. With these designed loss terms, the overall optimization objective can be formulated as:

$$\mathcal{L}_{\text{total}} = \mathcal{L}_{\text{RE}} + \lambda_{\text{DPO}} \mathcal{L}_{\text{DPO}} + \lambda_{\text{Anc}} \mathcal{L}_{\text{Anc}}, \quad (5)$$

where λ_{Anc} controls the influence of anchor loss \mathcal{L}_{Anc} .

3.3. Theoretical Analysis

In addition to empirical analysis, we build a theoretical framework to validate the effectiveness of C3PO. Let X denote the input, Y the ground truth response, and Z the reasoning trace. Note that $Y \rightarrow X \rightarrow Z$ is a Markov chain, where Z serves as the intermediate representation between input and output. Based on the Information Bottleneck theory (Tishby et al., 2000; Tishby & Zaslavsky, 2015; Shwartz-Ziv & Tishby, 2017), a well-trained model should:

- Minimize $\mathcal{I}(X; Z)$, *i.e.*, the mutual information between the input and intermediate representation. This urges the model to compress redundant information in the input, thereby simplifying the problem.
- Maximize $\mathcal{I}(Y; Z)$, *i.e.*, the mutual information between the ground truth and intermediate representation. This urges the model to retain task-relevant information necessary for producing the correct answer.

Overall, the Information Bottleneck objective is defined as

$$\mathcal{L}_{\text{IB}}(Z) = \mathcal{I}(X; Z) - \lambda_{\text{IB}} \mathcal{I}(Y; Z), \quad (6)$$

where $\lambda_{\text{IB}} > 0$ is a hyperparameter controlling the trade-off. A lower $\mathcal{L}_{\text{IB}}(Z)$ indicates a better trade-off between redundancy compression and predictive accuracy. In particular, we focus on the regime $\lambda_{\text{IB}} > 1$ to prioritize accuracy over compression, as suggested in Alemi et al. (2017).

Formally, we justify the effectiveness of our proposed two key operations (*i.e.*, CoT compression and enhancement) in reducing the IB objective by the following theorems:

Theorem 1 (Compression reduces IB). *Let the CoT Z be decomposed into Z_{ret} and Z_{trim} , where Z_{ret} denotes the retaining task-critical part, Z_{trim} represents the trimmed redundant part, $Z_{\text{ret}} \cup Z_{\text{trim}} = Z$ and $Z_{\text{ret}} \cap Z_{\text{trim}} = \emptyset$. Then, the IB objective satisfies*

$$\mathcal{L}_{\text{IB}}(Z) \geq \mathcal{L}_{\text{IB}}(Z_{\text{ret}}). \quad (7)$$

Theorem 2 (Enhancement reduces IB). *Let the CoT Z be refined to Z' via our reasoning-enhanced optimization, which supplements information about the ground truth Y . Then, the IB objective satisfies*

$$\mathcal{L}_{\text{IB}}(Z) > \mathcal{L}_{\text{IB}}(Z'). \quad (8)$$

The proofs are provided in Appendix A. Theorems 1 and 2 show that both compressing and enhancing the CoT reduce the model’s information bottleneck objective, which facilitates a more compact and accurate intermediate reasoning process for more reliable answers.

Table 1. Comparison of the proposed C3PO with competitive baselines on the CHAIR metric. We evaluate the performance on MSCOCO. C_S and C_I denotes CHAIR_S and CHAIR_I respectively.

Method	R1-Onevision		Orsta-R1		MM-Eureka		MM-R1		ThinkLite	
	$C_S \downarrow$	$C_I \downarrow$								
vanilla	36.7	8.2	40.7	8.5	44.0	8.6	37.0	7.4	41.7	7.8
RLAIF-V	39.0	8.3	39.7	7.6	41.3	8.5	38.7	7.5	40.3	7.5
OPA-DPO	36.7	7.7	41.7	8.2	41.3	7.7	36.3	7.2	40.0	7.9
C3PO	35.0	7.4	35.3	6.9	40.0	7.7	35.0	7.2	38.0	7.3

4. Experiments

This section provides comprehensive experiments on various MLRMs across different scenarios. Due to page limits, more experiments are provided in Appendix C.

4.1. Experimental Setup

Models and Datasets. To verify the effectiveness of our method, we conduct experiments on five representative MLRMs: Orsta-R1-7B (Ma et al., 2025), ThinkLite-7B (Wang et al., 2025), MM-Eureka-7B (Meng et al., 2025), MM-R1-7B (Leng et al., 2025), and R1-Onevision-7B (Yang et al., 2025a). To construct training data, we randomly sample 20k data pairs from the RLAIF-V dataset (Yu et al., 2025) as seed data. The CoT compression ratio is 90% by default. We apply a random masking ratio of 0.3 to the visual input for hallucination-inducing responses. More details, such as the designed *misleading prompt*, are in Appendix B.1.

Evaluation Benchmarks. We comprehensively evaluate the performance across a wide range of benchmarks. For hallucination evaluation, we consider (1) the CHAIR metric (Rohrbach et al., 2018), which evaluates object hallucinations in open-ended caption generation; (2) POPE (Li et al., 2023), a discriminative benchmark that evaluates object existence consistency via *yes/no* questions; (3) AMBER (Wang et al., 2023), a systematic benchmark designed to assess fine-grained hallucinations; (4) GPT-4 assisted Evaluation (Zhao et al., 2023) that uses GPT-4 series models to compute Sentence-level Hallucination Ratio (SHR) to detect fine-grained hallucinations. In addition, we evaluate the models on two widely used general-purpose benchmarks to assess their overall multimodal capabilities: (1) MME (Fu et al., 2025), a comprehensive benchmark measuring multiple dimensions of multimodal proficiency; and (2) MMBench (Liu et al., 2024), a multiple-choice benchmark probing complex multimodal comprehension and reasoning.

Baselines. Since there is no previous studies specifically address hallucination mitigation for MLRMs, we adapt two state-of-the-art (SOTA) training-based approaches originally designed for MLLMs as competitive baselines, including RLAIF-V (Yu et al., 2025) with iterative DPO and inference-time scaling and the powerful OPA-DPO (Yang et al., 2025b)

that employs on-policy DPO to ensure the alignment of the reference model with the preference data distribution

Implementation Details. In the first SFT stage, we employ Low-Rank Adaptation (LoRA) with a rank of $r = 8$ and a scaling factor of $\alpha = 16$ for 2 epochs with a learning rate of $5e^{-5}$ and a global batch size $B = 256$. For the subsequent DPO stage, we adopt a learning rate of $1e^{-6}$ and $B = 32$ for 2 epochs of training, with the KL penalty coefficient $\beta = 0.1$. As suggested in (Wang et al., 2024; Yang et al., 2025b), we set $\delta = 0$ in Eq. (4) and $\lambda_{\text{Anc}} = 1.0$ for the anchor loss \mathcal{L}_{Anc} in Eq. (5). For the hyperparameter λ_{DPO} , we conduct experiments to obtain the optimal value for each model in Appendix C. Following (Yang et al., 2025b; Yu et al., 2025), we adopt the greedy decoding for evaluation reproducibility. More details are provided in Appendix B.

4.2. Performance Evaluation

CHAIR Evaluation. Following (Yu et al., 2025; Yang et al., 2025b), we instruct the MLRMs to generate captions on 300 images from the MSCOCO validation set (Lin et al., 2014) and report results in Table 1. By effectively enhancing the reasoning process, the proposed framework consistently reduces hallucination across all MLRMs, significantly outperforming baselines. *E.g.*, C3PO achieves a 13.27% and 18.82% reduction of C_S and C_I on Orsta-R1, respectively.

Note that in contrast to consistent hallucination mitigation achieved by our method, baseline methods may even exacerbate hallucination in certain cases, *e.g.*, RLAIF-V on R1-Onevision and OPA-DPO on Orsta-R1. This phenomenon reveals the instability of transferring methods for MLLMs to the MLRM setting, further highlighting the necessity and effectiveness of the proposed method, which explicitly accounts for their unique reasoning process.

POPE Evaluation. POPE is another evaluation framework for object hallucination, which queries models with “Is there a *<object>* in the image?” to answer a *yes/no* question. These questions are further categorized into Random, Popular, and Adversarial based on the object type (see Appendix B.2 for details). We report the accuracy and F1 scores over 3,000 classification results in Table 2. The results indicate that the proposed method facilitates

Table 2. Comparison of the proposed C3PO with competitive baselines on the POPE benchmark (%).

Model	Method	Random		Popular		Adversarial	
		Accuracy	F1 score	Accuracy	F1 score	Accuracy	F1 score
MM-Eureka	<i>vanilla</i>	84.12	81.90	83.90	81.23	83.47	80.85
	RLAIF-V	83.81	81.46	83.70	80.89	83.27	80.47
	OPA-DPO	85.29	83.46	84.93	82.70	84.37	82.16
	C3PO	86.22	84.68	85.87	83.94	85.23	83.34
MM-R1	<i>vanilla</i>	84.85	82.83	84.47	82.04	83.97	81.56
	RLAIF-V	85.12	83.22	84.70	82.39	84.23	81.95
	OPA-DPO	85.33	83.52	85.00	82.79	84.50	82.31
	C3PO	86.91	85.57	86.37	84.68	85.57	83.91
ThinkLite	<i>vanilla</i>	83.23	80.63	83.03	79.97	82.77	79.72
	RLAIF-V	83.71	81.29	83.37	80.50	83.00	80.14
	OPA-DPO	85.02	83.07	84.70	82.34	84.10	81.77
	C3PO	85.98	84.37	85.63	83.63	84.97	83.00

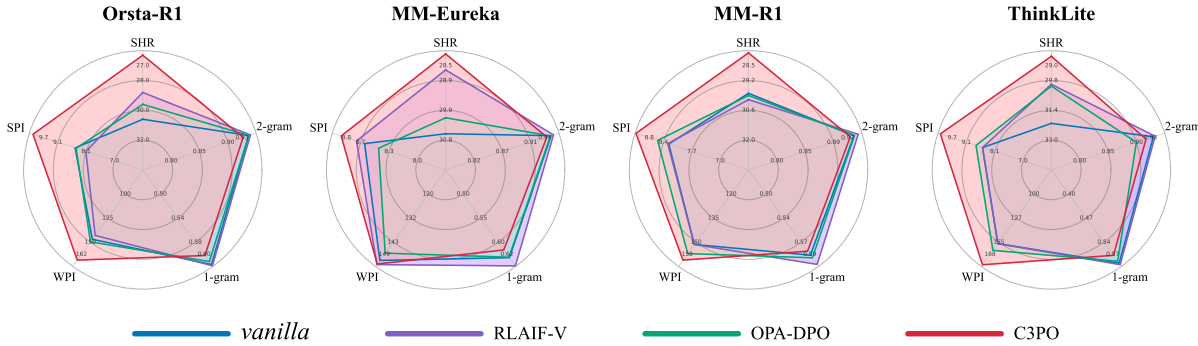


Figure 4. GPT-4 assisted benchmark. Sentence-level Hallucination Ratio (SHR) measures the hallucination degree. We also provide 1&2-gram, the number of sentences per image (SPI), and words per image (WPI). A larger radar area indicates better performance.

more effective reasoning and enables better perception of the images, substantially reducing hallucination rates across all three question types. Due to space limits, results for R1-Onevision and Orsta-R1 are provided in Appendix C.

GPT-4 Assisted Evaluation. While CHAIR and POPE are two widely used and reliable hallucination benchmarks, they focus exclusively on object hallucination and do not consider more complex positional, relational, or attribute hallucinations. To address this, we adopt the GPT-Assisted Benchmark (Zhao et al., 2023), an LLM-as-judge framework that comprehensively evaluates fine-grained hallucinations using the Visual Genome dataset (Krishna et al., 2017). Specifically, the MLRM first generates a description for a given image, and the GPT 4-series model is instructed to assess the hallucination level of the generated content based on fine-grained human annotations.

As shown in Figure 4, C3PO achieves strong overall performance across various MLRMs, significantly reducing

fine-grained hallucinations. For instance, C3PO reduces the SHR by 14.05% for Orsta-R1 compared to the *vanilla* model. Moreover, it substantially improves response detail (higher WPI and SPI), possibly benefiting from reasoning-enhanced training, which allows a more comprehensive and detailed perception to the visual input.

AMBER Evaluation. AMBER (Zhao et al., 2023) is another challenging benchmark designed to measure models’ multi-dimensional hallucinations, including existence, attribute, and relation hallucinations. Following (Yu et al., 2025), we focus on the discriminative part for an objective and reproducible evaluation and report accuracy and F1 scores on more than 15,000 carefully designed yes/no questions in Table 3. While baseline methods provide only limited improvements or even degrade the performance, the proposed C3PO consistently achieves improvements in hallucination mitigation, again demonstrating the necessity and effectiveness of the proposed framework.

Table 3. Comparison of the proposed C3PO with competitive baselines on the AMBER benchmark (%).

Method	R1-Onevision		Orsta-R1		MM-Eureka		MM-R1		ThinkLite	
	Acc. \uparrow	F1 \uparrow								
vanilla	81.52	86.54	82.94	87.31	83.27	87.15	84.38	88.20	82.25	86.96
RLAIF-V	80.99	84.97	83.14	87.50	83.46	87.49	84.17	88.11	82.31	87.04
OPA-DPO	80.71	85.30	83.58	87.67	83.72	87.59	84.76	88.51	83.02	87.36
C3PO	81.90	86.73	84.57	88.50	85.01	88.80	85.61	89.25	83.96	88.26

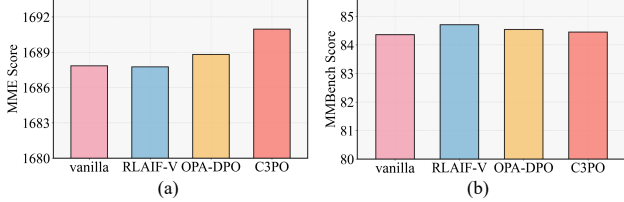


Figure 5. Performance on two general-purpose benchmarks.

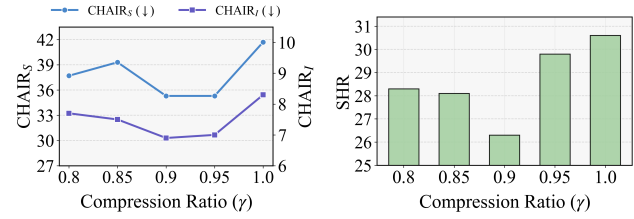
MME and MMBench Evaluations. In addition to hallucination benchmarks, we evaluate two popular general-purpose benchmarks using Orsta-R1 to measure the multimodal capabilities. MME provides a suite of fine-grained and multiple-choice questions across various categories. We align with (Huang et al., 2024) and report the overall perception score covering 10 multimodal sub-tasks. MMBench is another large-scale benchmark consisting of over 3,000 curated multiple-choice questions. We compute the average score across 20 complex tasks, including logical reasoning. As observed in Figure 5, the proposed reasoning-oriented strategy allows the model to maintain general capabilities and even bring improvements over the base model.

4.3. Ablation Study

In this section, we use Orsta-R1 as a representative model for ablation studies. See more ablation in Appendix C.

Ablation on the compression ratio. During the construction of the SFT data, γ is a critical hyperparameter that controls the number of remaining tokens. A larger γ may fail to sufficiently remove redundancy, while a smaller γ may discard informative tokens and thus degrade performance. As shown in Figure 6, $\gamma = 0.9$ achieves optimal performance on both CHAIR and GPT-4 assisted evaluations. Moreover, we observe that pruning rates smaller than 1 generally outperform the no pruning ($\gamma = 1$), again validating the effectiveness of our CoT compression strategy.

Ablation on the designed techniques. In addition to CoT compression, we then verify the effectiveness of the other proposed techniques. Specifically, we evaluate the designed loss functions \mathcal{L}_{RE} , \mathcal{L}_{DPO} , and \mathcal{L}_{Anc} , as well as the proposed Multimodal Hallucination-Inducing (MHI) strategy.


Figure 6. Ablation study of the compression ratio γ .

The results in Table 4 confirm the contribution of each component to the performance, validating the rationale behind our design choices. Notably, removing \mathcal{L}_{DPO} leads to a significant performance drop, showing the necessity of modeling the entire output distribution as a regularization.

Table 4. Ablation study of proposed techniques in C3PO under CHAIR and GPT-4 assisted benchmarks.

Method	CHAIR Eval		GPT-4 Eval SHR \downarrow
	$C_S \downarrow$	$C_I \downarrow$	
C3PO	35.3	6.9	26.3
w/o loss \mathcal{L}_{RE}	37.3	7.2	28.8
w/o loss \mathcal{L}_{DPO}	39.7	8.1	29.4
w/o loss \mathcal{L}_{Anc}	37.7	7.5	27.2
w/o MHI strategy	37.0	7.9	28.4

5. Conclusion

This work investigates the critical issue of hallucinations in MLRMs. We begin by analyzing two key factors contributing to hallucination emergence, based on which we propose C3PO, a two-stage training framework that first adopts SFT to remove redundancy in generated reasoning trajectories, and then explicitly enhances reasoning via contrastive preference optimization with carefully constructed preference pairs. We theoretically justify the proposed framework from the information bottleneck principle. Extensive experiments across diverse MLRMs and benchmarks validate its effectiveness and generality. We highlight that this work makes a pioneering step in mitigating hallucinations in MLRMs, deepening the understanding of the underlying mechanisms, and inspiring future studies on mitigation strategies.

Impact Statement

This paper makes an early step toward mitigating the serious hallucination issue in MLRMs. The goal is to advance the field of machine learning by improving the reliability of MLRM reasoning and reducing hallucinated outputs. There are many potential societal consequences of this line of research, most of which are consistent with those commonly associated with improving the robustness and trustworthiness of machine learning systems, and none that we believe require specific discussion here.

References

Alemi, A. A., Fischer, I., and Dillon, J. V. Deep variational information bottleneck. *International Conference on Learning Representations (ICLR)*, 2017.

Bai, S., Cai, Y., Chen, R., Chen, K., Chen, X., Cheng, Z., Deng, L., Ding, W., Gao, C., Ge, C., Ge, W., Guo, Z., Huang, Q., Huang, J., Huang, F., Hui, B., Jiang, S., Li, Z., Li, M., Li, M., Li, K., Lin, Z., Lin, J., Liu, X., Liu, J., Liu, C., Liu, Y., Liu, D., Liu, S., Lu, D., Luo, R., Lv, C., Men, R., Meng, L., Ren, X., Ren, X., Song, S., Sun, Y., Tang, J., Tu, J., Wan, J., Wang, P., Wang, P., Wang, Q., Wang, Y., Xie, T., Xu, Y., Xu, H., Xu, J., Yang, Z., Yang, M., Yang, J., Yang, A., Yu, B., Zhang, F., Zhang, H., Zhang, X., Zheng, B., Zhong, H., Zhou, J., Zhou, F., Zhou, J., Zhu, Y., and Zhu, K. Qwen3-vl technical report, 2025a. URL <https://arxiv.org/abs/2511.21631>.

Bai, S., Chen, K., Liu, X., Wang, J., Ge, W., Song, S., Dang, K., Wang, P., Wang, S., Tang, J., et al. Qwen2.5-vl technical report. *arXiv preprint arXiv:2502.13923*, 2025b.

Chen, X., Xu, J., Liang, T., He, Z., Pang, J., Yu, D., Song, L., Liu, Q., Zhou, M., Zhang, Z., et al. Do not think that much for 2+ 3=? on the overthinking of o1-like llms. *arXiv preprint arXiv:2412.21187*, 2024.

Dong, B., Ni, M., Huang, Z., Yang, G., Zuo, W., and Zhang, L. Mirage: Assessing hallucination in multimodal reasoning chains of mllm. *arXiv preprint arXiv:2505.24238*, 2025a.

Dong, Y., Liu, Z., Sun, H.-L., Yang, J., Hu, W., Rao, Y., and Liu, Z. Insight-v: Exploring long-chain visual reasoning with multimodal large language models. In *Proceedings of the Computer Vision and Pattern Recognition Conference*, pp. 9062–9072, 2025b.

Fang, H., Zhou, C., Kong, J., Gao, K., Chen, B., Liang, T., Ma, G., and Xia, S.-T. Grounding language with vision: A conditional mutual information calibrated decoding strategy for reducing hallucinations in lvlms. *Advances in Neural Information Processing Systems*, 2025.

Favero, A., Zancato, L., Trager, M., Choudhary, S., Perera, P., Achille, A., Swaminathan, A., and Soatto, S. Multi-modal hallucination control by visual information grounding. In *Proceedings of the IEEE/CVF Conference on Computer Vision and Pattern Recognition*, pp. 14303–14312, 2024.

Feng, S., Fang, G., Ma, X., and Wang, X. Efficient reasoning models: A survey. *arXiv preprint arXiv:2504.10903*, 2025.

Fu, C., Chen, P., Shen, Y., Qin, Y., Zhang, M., Lin, X., Yang, J., Zheng, X., Li, K., Sun, X., et al. Mme: A comprehensive evaluation benchmark for multimodal large language models. In *The Thirty-ninth Annual Conference on Neural Information Processing Systems Datasets and Benchmarks Track*, 2025.

Guo, D., Yang, D., Zhang, H., Song, J., Zhang, R., Xu, R., Zhu, Q., Ma, S., Wang, P., Bi, X., et al. Deepseek-r1: Incentivizing reasoning capability in llms via reinforcement learning. *arXiv preprint arXiv:2501.12948*, 2025.

Huang, Q., Dong, X., Zhang, P., Wang, B., He, C., Wang, J., Lin, D., Zhang, W., and Yu, N. Opera: Alleviating hallucination in multi-modal large language models via over-trust penalty and retrospection-allocation. In *Proceedings of the IEEE/CVF Conference on Computer Vision and Pattern Recognition*, pp. 13418–13427, 2024.

Jiang, C., Xu, H., Dong, M., Chen, J., Ye, W., Yan, M., Ye, Q., Zhang, J., Huang, F., and Zhang, S. Hallucination augmented contrastive learning for multimodal large language model. In *Proceedings of the IEEE/CVF Conference on Computer Vision and Pattern Recognition*, pp. 27036–27046, 2024.

Kojima, T., Gu, S. S., Reid, M., Matsuo, Y., and Iwasawa, Y. Large language models are zero-shot reasoners. *Advances in neural information processing systems*, 35: 22199–22213, 2022.

Krishna, R., Zhu, Y., Groth, O., Johnson, J., Hata, K., Kravitz, J., Chen, S., Kalantidis, Y., Li, L.-J., Shamma, D. A., et al. Visual genome: Connecting language and vision using crowdsourced dense image annotations. *International journal of computer vision*, 123(1):32–73, 2017.

Leng, S., Wang, J., Li, J., Zhang, H., Hu, Z., Zhang, B., Jiang, Y., Zhang, H., Li, X., Bing, L., et al. Mmr1: Enhancing multimodal reasoning with variance-aware sampling and open resources. *arXiv preprint arXiv:2509.21268*, 2025.

Li, G., Gao, Y., Li, Y., and Wu, Y. Thinkless: A training-free inference-efficient method for reducing reasoning redundancy. *arXiv preprint arXiv:2505.15684*, 2025.

Li, Y., Du, Y., Zhou, K., Wang, J., Zhao, W. X., and Wen, J.-R. Evaluating object hallucination in large vision-language models. *arXiv preprint arXiv:2305.10355*, 2023.

Lin, T.-Y., Maire, M., Belongie, S., Hays, J., Perona, P., Ramanan, D., Dollár, P., and Zitnick, C. L. Microsoft coco: Common objects in context. In *European conference on computer vision*, pp. 740–755. Springer, 2014.

Liu, C., Xu, Z., Wei, Q., Wu, J., Zou, J., Wang, X. E., Zhou, Y., and Liu, S. More thinking, less seeing? assessing amplified hallucination in multimodal reasoning models. *Advances in Neural Information Processing Systems*, 2025.

Liu, F., Lin, K., Li, L., Wang, J., Yacoob, Y., and Wang, L. Mitigating hallucination in large multi-modal models via robust instruction tuning. *arXiv preprint arXiv:2306.14565*, 2023.

Liu, Y., Duan, H., Zhang, Y., Li, B., Zhang, S., Zhao, W., Yuan, Y., Wang, J., He, C., Liu, Z., et al. Mmbench: Is your multi-modal model an all-around player? In *European conference on computer vision*, pp. 216–233. Springer, 2024.

Lu, P., Mishra, S., Xia, T., Qiu, L., Chang, K.-W., Zhu, S.-C., Tafjord, O., Clark, P., and Kalyan, A. Learn to explain: Multimodal reasoning via thought chains for science question answering. *Advances in Neural Information Processing Systems*, 35:2507–2521, 2022.

Ma, Y., Du, L., Shen, X., Chen, S., Li, P., Ren, Q., Ma, L., Dai, Y., Liu, P., and Yan, J. One rl to see them all: Visual triple unified reinforcement learning. *arXiv preprint arXiv:2505.18129*, 2025.

Meng, F., Du, L., Liu, Z., Zhou, Z., Lu, Q., Fu, D., Han, T., Shi, B., Wang, W., He, J., et al. Mm-eureka: Exploring the frontiers of multimodal reasoning with rule-based reinforcement learning. *arXiv preprint arXiv:2503.07365*, 2025.

Pan, Z., Wu, Q., Jiang, H., Xia, M., Luo, X., Zhang, J., Lin, Q., Rühle, V., Yang, Y., Lin, C.-Y., et al. Llmlingua-2: Data distillation for efficient and faithful task-agnostic prompt compression. In *Findings of the Association for Computational Linguistics ACL 2024*, pp. 963–981, 2024.

Rohrbach, A., Hendricks, L. A., Burns, K., Darrell, T., and Saenko, K. Object hallucination in image captioning. In *Proceedings of the 2018 Conference on Empirical Methods in Natural Language Processing*, pp. 4035–4045, 2018.

Shwartz-Ziv, R. and Tishby, N. Opening the black box of deep neural networks via information. *ArXiv*, 2017.

Tishby, N. and Zaslavsky, N. Deep learning and the information bottleneck principle. *Information Theory Workshop (ITW)*, 2015.

Tishby, N., Pereira, F. C., and Bialek, W. The information bottleneck method. *ArXiv*, 2000.

Wang, F., Zhou, W., Huang, J. Y., Xu, N., Zhang, S., Poon, H., and Chen, M. mdpo: Conditional preference optimization for multimodal large language models. In *Proceedings of the 2024 Conference on Empirical Methods in Natural Language Processing*, pp. 8078–8088, 2024.

Wang, J., Wang, Y., Xu, G., Zhang, J., Gu, Y., Jia, H., Yan, M., Zhang, J., and Sang, J. An llm-free multi-dimensional benchmark for mllms hallucination evaluation. *CoRR*, 2023.

Wang, X., Wei, J., Schuurmans, D., Le, Q., Chi, E., Narang, S., Chowdhery, A., and Zhou, D. Self-consistency improves chain of thought reasoning in language models. *arXiv preprint arXiv:2203.11171*, 2022.

Wang, X., Yang, Z., Feng, C., Lu, H., Li, L., Lin, C.-C., Lin, K., Huang, F., and Wang, L. Sota with less: Mcts-guided sample selection for data-efficient visual reasoning self-improvement. *arXiv preprint arXiv:2504.07934*, 2025.

Wei, J., Wang, X., Schuurmans, D., Bosma, M., Xia, F., Chi, E., Le, Q. V., Zhou, D., et al. Chain-of-thought prompting elicits reasoning in large language models. *Advances in neural information processing systems*, 35:24824–24837, 2022.

Xia, H., Leong, C. T., Wang, W., Li, Y., and Li, W. TokenSkip: Controllable chain-of-thought compression in LLMs. In Christodoulopoulos, C., Chakraborty, T., Rose, C., and Peng, V. (eds.), *Proceedings of the 2025 Conference on Empirical Methods in Natural Language Processing*, pp. 3351–3363, Suzhou, China, November 2025. Association for Computational Linguistics. ISBN 979-8-89176-332-6. doi: 10.18653/v1/2025.emnlp-main.165. URL <https://aclanthology.org/2025.emnlp-main.165/>.

Xing, Y., Li, Y., Laptev, I., and Lu, S. Mitigating object hallucination via concentric causal attention. *Advances in neural information processing systems*, 37:92012–92035, 2024.

Yang, Y., He, X., Pan, H., Jiang, X., Deng, Y., Yang, X., Lu, H., Yin, D., Rao, F., Zhu, M., et al. R1-onevision: Advancing generalized multimodal reasoning through cross-modal formalization. *arXiv preprint arXiv:2503.10615*, 2025a.

Yang, Z., Luo, X., Han, D., Xu, Y., and Li, D. Mitigating hallucinations in large vision-language models via dpo: On-policy data hold the key. In *Proceedings of the Computer Vision and Pattern Recognition Conference*, pp. 10610–10620, 2025b.

Yin, S., Fu, C., Zhao, S., Xu, T., Wang, H., Sui, D., Shen, Y., Li, K., Sun, X., and Chen, E. Woodpecker: Hallucination correction for multimodal large language models. *Science China Information Sciences*, 67(12):220105, 2024.

Yu, Q., Li, J., Wei, L., Pang, L., Ye, W., Qin, B., Tang, S., Tian, Q., and Zhuang, Y. Hallucidocor: Mitigating hallucinatory toxicity in visual instruction data. In *Proceedings of the IEEE/CVF Conference on Computer Vision and Pattern Recognition*, pp. 12944–12953, 2024a.

Yu, T., Yao, Y., Zhang, H., He, T., Han, Y., Cui, G., Hu, J., Liu, Z., Zheng, H.-T., Sun, M., et al. Rlhf-v: Towards trustworthy mllms via behavior alignment from fine-grained correctional human feedback. In *Proceedings of the IEEE/CVF Conference on Computer Vision and Pattern Recognition*, pp. 13807–13816, 2024b.

Yu, T., Zhang, H., Li, Q., Xu, Q., Yao, Y., Chen, D., Lu, X., Cui, G., Dang, Y., He, T., et al. Rlaif-v: Open-source ai feedback leads to super gpt-4v trustworthiness. In *Proceedings of the Computer Vision and Pattern Recognition Conference*, pp. 19985–19995, 2025.

Zhang, R., Zhang, B., Li, Y., Zhang, H., Sun, Z., Gan, Z., Yang, Y., Pang, R., and Yang, Y. Improve vision language model chain-of-thought reasoning. In *Proceedings of the 63rd Annual Meeting of the Association for Computational Linguistics (Volume 1: Long Papers)*, pp. 1631–1662, 2025.

Zhang, Z., Zhang, A., Li, M., Zhao, H., Karypis, G., and Smola, A. Multimodal chain-of-thought reasoning in language models. *arXiv preprint arXiv:2302.00923*, 2023.

Zhao, Z., Wang, B., Ouyang, L., Dong, X., Wang, J., and He, C. Beyond hallucinations: Enhancing lylms through hallucination-aware direct preference optimization. *arXiv preprint arXiv:2311.16839*, 2023.

A. Proofs for Theorems

Here we prove our theorems in Section 3.3.

Theorem 1 (Compression reduces IB). *Let the CoT Z be decomposed into Z_{ret} and Z_{trim} , where Z_{ret} denotes the retaining task-critical part, Z_{trim} represents the trimmed redundant part, $Z_{\text{ret}} \cup Z_{\text{trim}} = Z$ and $Z_{\text{ret}} \cap Z_{\text{trim}} = \emptyset$. Then, the IB objective satisfies*

$$\mathcal{L}_{\text{IB}}(Z) \geq \mathcal{L}_{\text{IB}}(Z_{\text{ret}}). \quad (9)$$

Proof. According to $Z = Z_{\text{ret}} \cup Z_{\text{trim}}$ and the chain rule of mutual information, we have

$$\begin{aligned} \mathcal{I}(X; Z) &= \mathcal{I}(X; Z_{\text{ret}}) + \mathcal{I}(X; Z_{\text{trim}}|Z_{\text{ret}}), \\ \mathcal{I}(Y; Z) &= \mathcal{I}(Y; Z_{\text{ret}}) + \mathcal{I}(Y; Z_{\text{trim}}|Z_{\text{ret}}). \end{aligned} \quad (10)$$

When Z_{ret} is given, Z_{trim} can be relevant to the input X but irrelevant to the ground truth Y , because our compressor only trims low-importance words without contributions to final predictions (see Appendix E.1). Therefore

$$\mathcal{I}(X; Z_{\text{trim}}|Z_{\text{ret}}) \geq 0, \quad \mathcal{I}(Y; Z_{\text{trim}}|Z_{\text{ret}}) = 0. \quad (11)$$

(10) and (11) yield

$$\mathcal{I}(X; Z) \geq \mathcal{I}(X; Z_{\text{ret}}), \quad \mathcal{I}(Y; Z) = \mathcal{I}(Y; Z_{\text{ret}}). \quad (12)$$

Then we conclude that

$$\begin{aligned} \mathcal{L}_{\text{IB}}(Z) &= \mathcal{I}(X; Z) - \lambda_{\text{IB}} \mathcal{I}(Y; Z), \\ &\geq \mathcal{I}(X; Z_{\text{ret}}) - \lambda_{\text{IB}} \mathcal{I}(Y; Z_{\text{ret}}), \\ &= \mathcal{L}_{\text{IB}}(Z_{\text{ret}}). \end{aligned} \quad (13)$$

□

Theorem 2 (Enhancement reduces IB). *Let the CoT Z be refined to Z' via our reasoning-enhanced optimization, which supplements information about the ground truth Y . Then, the IB objective satisfies*

$$\mathcal{L}_{\text{IB}}(Z) > \mathcal{L}_{\text{IB}}(Z'). \quad (14)$$

Proof. Note that the correct answer Y is contained within the input X , which implies

$$\mathcal{I}(X; Z) = \mathcal{I}(X, Y; Z), \quad \mathcal{I}(X; Z') = \mathcal{I}(X, Y; Z'). \quad (15)$$

In addition, according to the chain rule of mutual information, we have

$$\begin{aligned} \mathcal{I}(X; Z) &= \mathcal{I}(Y; Z) + \mathcal{I}(X; Z|Y), \\ \mathcal{I}(X; Z') &= \mathcal{I}(Y; Z') + \mathcal{I}(X; Z'|Y). \end{aligned} \quad (16)$$

Our reasoning-enhanced optimization guides the CoT towards the correct answer, thereby reducing the uncertainty of Y when Z' is given. Formally, it makes

$$\mathcal{H}(Y|Z) > \mathcal{H}(Y|Z'), \quad (17)$$

where \mathcal{H} is Shannon entropy to quantify uncertainty. Then

$$\begin{aligned} \mathcal{I}(Y; Z) &= \mathcal{H}(Y) - \mathcal{H}(Y|Z), \\ &< \mathcal{H}(Y) - \mathcal{H}(Y|Z'), \\ &= \mathcal{I}(Y; Z'). \end{aligned} \quad (18)$$

The information supplemented to Z' by our reasoning-enhanced optimization is contained within Y , which implies

$$\mathcal{H}(Z'|Z, Y) = 0. \quad (19)$$

Then we have

$$\begin{aligned} \mathcal{I}(X; Z'|Y) &\leq \mathcal{I}(X; Z, Z'|Y), \\ &= \mathcal{I}(X; Z|Y) + \mathcal{I}(X; Z'|Z, Y), \\ &\leq \mathcal{I}(X; Z|Y) + \mathcal{H}(Z'|Z, Y), \\ &= \mathcal{I}(X; Z|Y). \end{aligned} \quad (20)$$

Recall that we focus on $\lambda_{\text{IB}} > 1$ to prioritize accuracy over compression. Then we conclude that

$$\begin{aligned} \mathcal{L}_{\text{IB}}(Z) &= \mathcal{I}(X; Z) - \lambda_{\text{IB}} \mathcal{I}(Y; Z), \\ &= \mathcal{I}(Y; Z) + \mathcal{I}(X; Z|Y) - \lambda_{\text{IB}} \mathcal{I}(Y; Z), \\ &= \mathcal{I}(X; Z|Y) - (\lambda_{\text{IB}} - 1) \mathcal{I}(Y; Z), \\ &> \mathcal{I}(X; Z'|Y) - (\lambda_{\text{IB}} - 1) \mathcal{I}(Y; Z'), \\ &= \mathcal{I}(Y; Z') + \mathcal{I}(X; Z'|Y) - \lambda_{\text{IB}} \mathcal{I}(Y; Z'), \\ &= \mathcal{I}(X; Z') - \lambda_{\text{IB}} \mathcal{I}(Y; Z'), \\ &= \mathcal{L}_{\text{IB}}(Z'). \end{aligned} \quad (21)$$

□

B. Experimental Details

B.1. Data Construction

We randomly sample 20k image-question pairs from the RLAIF-V (Yu et al., 2025) dataset. Each instance provides an image v , a question x , and a reference answer y_{GT} .

SFT Dataset Construction. For each instance (v, x) , we query the target backbone to generate a structured response that contains an explicit CoT and a final answer. The output is parsed into an original reasoning trace z_{Gen} and an original answer y_{Gen} based on the `<think>` and `<answer>` tags. We apply LLMlingua-2 to filter redundant tokens in reasoning traces. By setting the compression ratio to $\gamma = 0.9$, we obtain the compressed reasoning chain $z' = \mathcal{C}(z; \gamma)$. Our SFT data is constructed directly from the

compressed reasoning trace paired with the model’s original answer. This design reduces redundant textual tokens in CoT, increasing the relative salience of visually relevant evidence during training. We train a reference model using this dataset via SFT, which subsequently serves as the generator for all negative samples in the preference learning stage.

Preference Dataset Construction. To construct the preference dataset, we employ a stronger evaluator Qwen3-VL-30B-Instruct to minimally refine the original reasoning trace and subsequently apply LLMlingua-2 to compress it, yielding the final corrected reasoning chain z_{Rev} . The goal of this step is to correct factual inconsistencies with image content while remaining faithful to the model’s stylistic characteristics and reasoning structure. We follow the revision prompt designed in (Yang et al., 2025b), the key refinement instruction is presented as follows:

Refinement Prompt:

Your role is as a discerning assistant tasked with evaluating and refining responses for multimodal tasks. Upon being presented with a question that requires the interpretation of both text and images, you will receive two distinct responses. The first is crafted by our sophisticated multimodal model, while the second represents an approximate ideal answer—it may be incomplete or incorrect. You will also be provided with the images pertinent to the question. Your objective is to meticulously assess these responses. You are to enhance the model-generated response by making precise, minimal modifications that bring it into closer alignment with both the image and the approximate ideal answer. Your revisions should preserve the integrity of the original response as much as possible.

We then construct the positive sample by concatenating this refined chain with the ground truth answer: $z_{\text{Rev}} \parallel y_{\text{GT}}$. This ensures that the positive sample acts as a gold standard, being both factually accurate regarding the visual content and structurally optimized for concise and efficient reasoning. For each training instance (v, x) , we pair the positive sample with three distinct negative samples derived from the reference model. These negatives comprise: (i) a *natural negative*, generated directly by the reference model given the original image and question, capturing the model’s intrinsic tendency to generate non-factual content; (ii) a *visually induced negative*, elicited by applying a random masking ratio of 0.3 to the visual tokens, which forces the model to hallucinate based on language priors due to incomplete visual information; (iii) an *instruction-induced negative*, crafted by appending a specific system prompt that explicitly steers the model towards fabrication:

Misleading Prompt:

Generate a response to the question about the image. Focus on using your language prior to creating a plausible-sounding reasoning trace and answer, but intentionally introduce hallucinations—details that seem related to the image but are not actually supported by it. Ignore the image content when necessary to make the response imaginative yet coherent.

B.2. Evaluation Benchmarks

Object HalBench Evaluations. To rigorously assess object-level hallucinations in open-ended image description, the CHAIR (Caption Hallucination Assessment with Image Relevance) metric is adopted. This metric quantifies the discrepancy between objects generated in captions and those present in the ground-truth annotations. Both instance-level (CHAIR_I) and sentence-level (CHAIR_S) scores are reported, where lower values indicate a higher degree of factual consistency. The mathematical formulations for these two variants are defined as follows:

$$C_I = \frac{|\text{hallucinated objects}|}{|\text{all mentioned objects}|}$$

$$C_S = \frac{|\text{captions with hallucinated objects}|}{|\text{all captions}|}$$

AMBER Evaluations. AMBER establishes a versatile framework for evaluating hallucinations in generative and discriminative scenarios. Following (Yu et al., 2025), we consider the discriminative task to assess fine-grained visual grounding for objective and reproducible evaluation. This task formulates hallucination assessment as a rigorous binary classification problem, probing the model with specific “Yes/No” queries to verify visual facts. It comprehensively covers three dimensions of hallucination: (i) *Existence*, verifying the presence of specific objects; (ii) *Attribute*, evaluating detailed properties including object states, counts, and actions; and (iii) *Relation*, assessing spatial relationships and interactions between objects. We report both Accuracy and F1 scores to quantify the model’s ability to distinguish truthful details from fabrications.

GPT-4 Assisted Evaluations. To quantify the degree of hallucination in detailed image descriptions, the Sentence-level Hallucination Ratio (SHR) is adopted. Following established protocols, models are prompted to describe images from the Visual Genome dataset (Krishna et al., 2017) in detail. The mini version of GPT-4o is utilized as a cost-effective and capable evaluator to identify contradictory statements in the generated text compared to the ground-truth annotations provided by the Visual Genome.

Table 5. Additional performance comparison on the POPE benchmark with Orsta-R1 and R1-Onevision backbones.

Model	Method	Random		Popular		Adversarial	
		Accuracy	F1 score	Accuracy	F1 score	Accuracy	F1 score
R1-Onevision	<i>vanilla</i>	83.64	81.82	82.80	80.59	81.93	79.81
	RLAIF-V	82.85	81.03	81.60	79.45	81.57	79.42
	OPA-DPO	83.85	82.28	82.57	80.67	82.03	80.19
	C3PO	83.88	82.66	82.53	81.01	82.37	80.87
Orsta-R1	<i>vanilla</i>	85.15	83.29	84.70	82.43	84.13	81.90
	RLAIF-V	85.95	84.32	85.37	83.36	84.57	82.61
	OPA-DPO	86.36	84.88	85.80	83.95	84.90	83.10
	C3PO	86.98	85.67	86.27	84.62	85.03	83.45

POPE Evaluations. To eliminate the ambiguity often found in free-form generation metrics, the Polling-based Object Probing Evaluation (POPE) reformulates hallucination assessment as a strict binary verification task. An equal distribution of positive and negative samples is enforced to eliminate the influence of prior label frequency. The evaluation includes three distinct difficulty levels: (i) *random* sampling serves as a standard baseline; (ii) *popular* sampling utilizes frequent categories to test resistance against popularity bias; and (iii) *adversarial* sampling employs co-occurring objects to challenge fine-grained visual discrimination. We report Accuracy and F1 scores to evaluate the reliability of object verification across these diverse settings.

MME and MMBench Evaluations. To ensure that the hallucination mitigation strategy does not compromise general multimodal capabilities, we conduct evaluations on two comprehensive benchmarks. MME is employed to assess a wide spectrum of perception and cognition tasks. By employing a suite of binary-choice questions with a consistent answer format, MME facilitates a precise measurement of a model’s ability to remain faithful to visual content. MMBench is utilized to evaluate complex multimodal comprehension across 20 distinct ability dimensions ranging from basic perception to high-level reasoning. To ensure robustness, it introduces the CircularEval strategy, which requires consistent predictions across multiple permutations of choices to eliminate the influence of random guessing. Together, these evaluations provide an effective validation of the model’s ability to preserve general multimodal understanding and instruction-following proficiency.

C. Additional Results

POPE evaluation on more MLRMs. As a supplement to the main text, we report POPE results on additional MLRMs, including R1-Onevision and Orsta-R1. The quantitative results in Table 5 further corroborate the effectiveness of our method in mitigating object hallucinations, outperforming

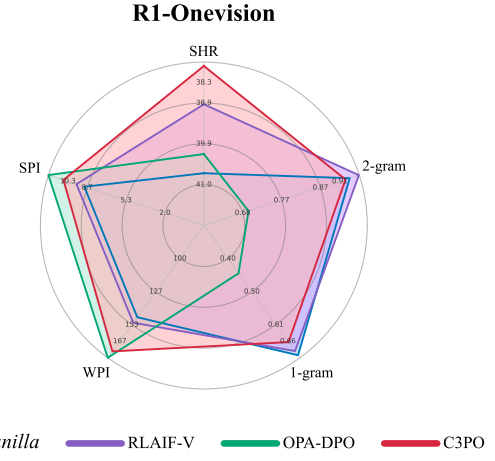


Figure 7. GPT-4 assisted benchmark results for R1-Onevision. Metrics include Sentence-level Hallucination Ratio (SHR), 1&2-gram, sentences per image (SPI), and words per image (WPI). A larger radar area indicates better performance.

baseline methods. This validates the necessity and efficacy of our CoT compression and preference optimization.

GPT-4 assisted evaluation on R1-Onevision. We further supplement the GPT-4 assisted benchmark results on R1-Onevision. As illustrated in Figure 7, the proposed C3PO significantly outperforms existing SOTA baselines. For instance, in comparison with competitive baseline OPA-DPO, C3PO attains a relative improvement of 5.7% on the SHR hallucination metric while maintaining comparable text fluency. The results indicate that the proposed redundant CoT token compression, combined with reasoning-enhanced contrastive preference optimization, synergistically suppresses hallucinations without compromising generation quality.

Ablation on preference optimization and SFT. To evaluate the effectiveness of the preference optimization, we design a variant that undergoes only SFT on compressed text, without subsequent preference optimization. As demonstrated

Table 6. Ablation study of C3PO on the preference optimization.

Model	Method	CHAIR Eval		GPT-4 Eval SHR \downarrow
		$C_S \downarrow$	$C_I \downarrow$	
R1-Onevision	C3PO	35.0	7.4	37.9
	w/o DPO	40.0	7.7	36.7
	vanilla	36.7	8.2	40.7
Orsta-R1	C3PO	35.3	6.9	26.3
	w/o DPO	39.7	7.7	29.2
	vanilla	40.7	8.5	30.6
MM-Eureka	C3PO	40.0	7.7	28.1
	w/o DPO	40.7	8.3	29.3
	vanilla	44.0	8.6	30.6
MM-R1	C3PO	35.0	7.2	27.9
	w/o DPO	35.3	6.9	31.0
	vanilla	37.0	7.4	29.8
ThinkLite	C3PO	38.0	7.3	28.5
	w/o DPO	41.3	7.2	29.9
	vanilla	41.7	7.8	32.1

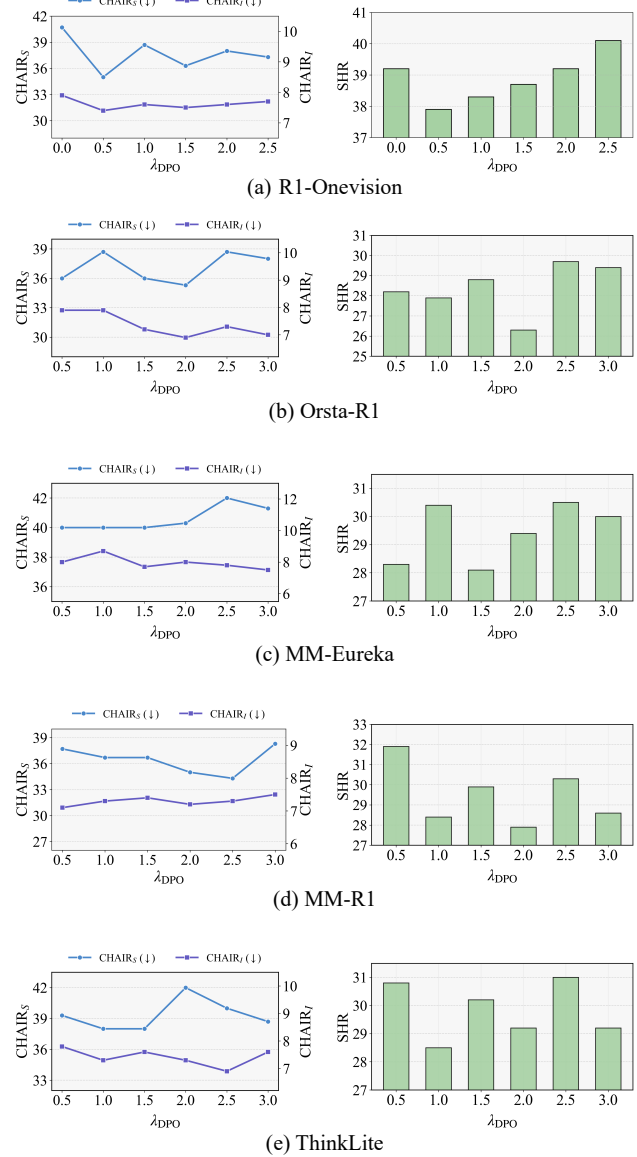
in Table 6, supervised fine-tuning on compressed text already leads to notable improvements across both evaluation benchmarks. Building upon this foundation, C3PO further achieves reductions of 4.4 and 2.9 in C_S and SHR when equipped with the proposed powerful preference optimization. Overall, these results indicate that the synergy between CoT token compression and DPO allows C3PO to achieve stronger performance gains.

Ablation on the hyperparameter λ_{DPO} . The value of λ_{DPO} is a critical hyperparameter as it controls the contribution of \mathcal{L}_{DPO} during optimization. We evaluate the performance under various values of λ_{DPO} in Figure 8 to select the optimal value for each MRLM. The results reveal that different models exhibit distinct optimal choices of λ_{DPO} . In particular, we comprehensively consider the performance on both benchmarks to select the optimal values $[0.5, 2.0, 1.5, 2.0, 1.0]$ for R1-Onevision, Orsta-R1, MM-Eureka, MM-R1, ThinkLite, respectively.

D. Related Work

D.1. Multimodal Large Reasoning Models

Reasoning has become a prevalent paradigm in LLMs, as the thinking process can significantly enhance complex problem solving with structured intermediate inference steps (Wei et al., 2022; Kojima et al., 2022; Wang et al., 2022). Recent studies extend this paradigm to multimodal models and introduce Multimodal Large Reasoning Models (MLRMs) that conduct an extra reasoning step (Lu et al., 2022; Zhang et al., 2023). To acquire such capabilities, prevalent approaches typically incorporate CoT supervision via supervised fine-tuning (SFT) or reinforcement learning (RL).


Figure 8. Ablation study on the weight factor λ_{DPO} of \mathcal{L}_{DPO} across different MRLMs.

Early works, including RLHF-V (Yu et al., 2024b), LLaVA-Reasoner (Zhang et al., 2025), and Insight-V (Dong et al., 2025b), primarily leveraged large-scale CoT-style datasets combined with preference optimization to align model behaviors with reliable reasoning patterns. Recent MRLMs typically follow two training paradigms: (i) two-stage SFT + RL strategy (e.g., R1-OneVision (Yang et al., 2025a)). (ii) direct large-scale RL approach (e.g., ThinkLite-VL (Wang et al., 2025), MM-Eureka (Meng et al., 2025)). During the RL stage, Group Relative Policy Optimization (GRPO) (Guo et al., 2025) is commonly adopted as an effective optimization algorithm for establishing reasoning capability.

D.2. Hallucination in MLRMs

Multimodal hallucination, which indicates that generated responses are semantically coherent but contradict the visual input, has been a notorious challenge for multimodal models. Existing mitigation strategies for regular MLLMs can be broadly grouped into training-free and training-based approaches. Training-free methods generally utilize prompting strategies, post-hoc correction, and improved decoding strategies to mitigate visual inconsistencies during inference (Xing et al., 2024; Yin et al., 2024; Huang et al., 2024; Fang et al., 2025). Training-based approaches enhance output faithfulness by modifying the training pipeline via data curation, SFT, and reinforcement learning (Yu et al., 2024a; Liu et al., 2023; Jiang et al., 2024; Zhao et al., 2023; Yu et al., 2025; Yang et al., 2025b).

The hallucination issue becomes even more prominent in MLRMs as longer reasoning traces shift attention away from image-grounded evidence, amplifying MLRMs’ reliance on language priors during generation. Liu et al. (2025) design a systematic benchmark to evaluate the hallucination behaviors of MLRMs and investigate influential factors. Dong et al. (2025a) focus on self-contradictory hallucinations in reasoning chains and introduces a dedicated benchmark that targets reasoning-stage failures. Despite the progress, mitigation strategies for MLRMs in general tasks remain largely unexplored. Existing algorithms are primarily designed for conventional MLLMs and do not account for the distinctive reasoning properties of MLRMs. In this paper, we present an effective mitigation framework tailored to MLRMs by explicitly enhancing their reasoning process.

E. Visualization Results

This section presents visualization results to provide a more intuitive understanding. We first show results of token pruning to demonstrate the rationality of our compression strategy. Then, we provide qualitative comparisons that confirm the superiority of C3PO in mitigating hallucinations.

E.1. Visualization of pruned CoTs.

We visualize the pruned reasoning traces at a mask ratio of 10% in Figure 9. The text marked in red indicates tokens identified as low-importance and are removed during the compression phase. As observed, the removed tokens are predominantly redundant function words (e.g., “that”, “is”, “the”) that contribute little semantic content and are irrespective of the final response. By stripping away these low-information redundancies, our approach forms a more compact and signal-efficient CoT representation that retains task-relevant information while suppressing noise.

E.2. Visualization of Hallucination Mitigation.

The qualitative comparisons in Figure 10 and Figure 11 reveal that baseline methods tend to exhibit hallucinations due to unreliable and low-quality reasoning. In contrast, C3PO conducts compact and reliable thinking and successfully provides the correct answer, effectively suppressing hallucinations for MLRMs.



Instruction

Explain the image's various components in depth.

Pruned CoTs: The image shows a natural outdoor setting with several components that contribute to the overall scenery: 1. Pathway: There is a central pathway made of a natural material, possibly packed earth or stone, which winds through the landscape. It suggests a walkway designed for exploration or recreational purposes. 2. Vegetation: The area is rich with various types of plants. On the left side, there are tall, slender grasses that add texture and movement to the scene. On the right, there are taller shrubs or small trees with golden-yellow flowers, contributing to the seasonal aesthetics. 3. Trees: There are large trees in the background that provide a sense of depth and scale. These trees are leafy and appear to be mature, suggesting that this is a well-established area. 4. Signpost: In the mid-right of the image, there is a signpost which might indicate directions, information about the plants or the route, or it could be a boundary marker. 5. Lighting: The lighting in the image indicates that the photograph was taken during the day under clear weather conditions. The sunlight seems to be illuminating the scene from the upper left, creating a play of light and shadow. 6. Sky: The sky is visible at the top of the image and appears clear with a light blue tone, suggesting a sunny day without visible clouds. All these elements together create a serene and inviting natural environment, possibly a park, botanical garden, or a nature reserve.



Instruction

Detail the image's components with particular focus on each entity.

Pruned CoTs : The image depicts a rural scene with two horses in the foreground, a fence separating them from a field, and a cluster of houses and trees in the background. Here's a breakdown of the components: 1. Foreground (Left Horse): This is the horse on the left side of the image. It appears to be dark in color. It is standing in a field with a fence in front of it. 2. Foreground (Right Horse): This is the horse on the right side of the image. It appears to be dark in color as well. It is standing in the same field with a fence in front of it. 3. Field: The ground where the horses are standing. It looks grassy with some patches of dirt. 4. Fence: A line of posts and wires runs horizontally across the image, separating the foreground from the background. 5. Background (Houses): There are multiple houses visible, partially obscured by trees. They appear to be two-story buildings with sloped roofs. 6. Background (Trees): Numerous trees are visible in the background, some with bare branches, suggesting it might be winter or early spring. There is also a taller tree to the far right. 7. Sky: The sky is not fully visible but appears to be clear and bright, suggesting daytime.

Figure 9. Visualization of the pruned CoTs.



Question

Is there a sun in this image?

Vanilla:<think>The image shows a person and a giraffe in an outdoor setting with a bright sky. The lighting suggests it is daytime, and the shadows cast by the person and the giraffe indicate the presence of a light source, **which is likely the sun**. The sky appears clear, **which is typical for a sunny day**.</think><answer>Yes</answer>

RLAIF-V:<think>The image shows a person standing next to a giraffe in a grassy area with trees in the background. The lighting in the image appears to be natural daylight, which **suggests that the sun is likely present**, even though it is not directly visible in the image. The shadows cast by the person and the giraffe **indicate that the sun is shining from a direction that is not directly visible in the frame**.</think><answer>Yes</answer>

OPA-DPO:<think>The image shows a man and a giraffe in a grassy area, but the sun is not visible in the image. However, the presence of shadows and the brightness of the scene **suggest that the sun is likely shining**. **Therefore, it is possible that the sun is in the image**.</think><answer>Yes, there is a sun in the image.</answer>

C3PO:<think>image shows a bright, clear sky with no visible sun. lighting suggests it is daytime, but sun itself is not directly visible in the image.</think><answer>No</answer>



Question

Is there a slippers in this image?

Vanilla:<think>The image shows a person sleeping on a bed with two dogs. The person appears to be wearing slippers, **which are visible at the bottom of the image**. The slippers are gray and are placed near the person's feet.</think><answer>Yes</answer>

RLAIF-V:<think>Upon analyzing the image, there is a person lying on a bed with two dogs. The person appears to be wearing slippers, **which are visible at the bottom of the image**. The slippers are gray and are placed near the person's feet.</think><answer>Yes</answer>

OPA-DPO:<think>The image shows a person sleeping on a bed with two dogs. **The person appears to be wearing slippers, which are visible at the bottom of the image**. The slippers are gray and are placed near the person's feet. The dogs are lying on the bed, one of them is looking directly at the camera, and the other is looking to the side. The setting appears to be a bedroom with a bed and curtains in the background. </think><answer>Yes, there is a pair of slippers visible in the image.</answer>

C3PO:<think>image shows a person sleeping on a bed with two dogs. bed has white sheets and a beige blanket. no visible slippers in the image. focus is on person, dogs, and bedding.</think><answer>No</answer>

Figure 10. Visualization results comparing our C3PO and other methods. Hallucinations are marked in red.



Question

Is there a cloud in this image?

Vanilla:<think> The image shows a train on a railway track surrounded by greenery. The sky is visible in the background and appears to be overcast, suggesting the presence of clouds. There are no distinct clouds visible, but the overall appearance of the sky indicates cloud cover. Therefore, it is reasonable to conclude that there are clouds in the image. </think><answer> Yes</answer>

RLAIF-V:<think> The image shows a train on a railway track surrounded by greenery. The sky is visible in the background, and it appears to be overcast, which suggests the presence of clouds. However, the image does not provide a clear view of individual clouds, only the general appearance of the sky. Given the overcast condition, it is reasonable to infer that there are clouds present, even if they are not distinctly visible.</think> <answer> Yes</answer>

OPA-DPO:<think> The image shows a train traveling through a lush, green landscape. The sky is visible in the background and appears to be overcast, suggesting the presence of clouds. There are no distinct shapes or features that would indicate the absence of clouds. </think> <answer> Yes, there is a cloud in the image.</answer>

C3PO:<think> image shows a train on a railway track surrounded by greenery. sky is visible in the background, appears to be overcast with no distinct clouds. lighting suggests a cloudy day, but no specific cloud formations can be identified. Therefore, presence of cloud cannot be confirmed with certainty from the image alone.</think><answer>No</answer>



Question

Is there a glacier in this image?

Vanilla:<think> The image shows two polar bears standing on what appears to be a large piece of ice. The ice looks expansive and is situated in a body of water, which is characteristic of a glacier or a large ice floe. The presence of the ice in a body of water suggests it could be part of a glacier or an ice floe from a larger glacier.</think><answer> Yes</answer>

RLAIF-V: RLAIF-V:<think> The image shows two polar bears standing on a large piece of ice. Glaciers are typically much larger and more permanent features of the landscape, often found in mountainous regions or at higher altitudes. The ice in the image looks more like a chunk of sea ice, which is common in polar regions where polar bears are found. Therefore, it is reasonable to conclude that the image does not depict a glacier.</think><answer> Yes</answer>

OPA-DPO: OPA-DPO:<think> The image shows two polar bears standing on what appears to be a large piece of ice. The ice looks like it could be a glacier or a large ice floe, which is a piece of floating ice that has broken off from a glacier. The presence of the polar bears and the icy environment suggest that this is a cold, Arctic-like setting where glaciers are common. </think> <answer> Yes, there is a glacier in the image.</answer>

C3PO:<think> image shows two polar bears standing on a large expanse of ice. ice appears to be floating on water, is characteristic of a glacier or ice floe. ice is not a glacier itself but rather a large piece of ice floating in water, is often referred to as an ice floe. presence of water and the way ice is floating suggest it is not a glacier.</think><answer> No</answer>

Figure 11. Visualization results comparing our C3PO and other methods. Hallucinations are marked in red.